

# Leptogenesis assisted by scalar decays

Jun-Yu Tong, Zhao-Huan Yu,<sup>\*</sup> and Hong-Hao Zhang<sup>†</sup>

*School of Physics, Sun Yat-Sen University, Guangzhou 510275, China*

We present a pragmatic approach to lower down the mass scale of right-handed neutrinos in leptogenesis by introducing a scalar decaying to right-handed neutrinos. The key point of our proposal is that the out-of-equilibrium decays of the scalar provide an additional source for right-handed neutrinos and hence the lepton asymmetry. This mechanism works well at low temperatures when the washout of the generated lepton asymmetry is suppressed. Thus, the lepton asymmetry can be effectively produced despite the washout effect is strong or not. Through a comprehensive analysis, we demonstrate that such a scalar-assisted leptogenesis can typically decrease the viable right-handed neutrino mass scale by two to four orders of magnitude.

## CONTENTS

I. Introduction	2
II. Model	3
III. Boltzmann equations	7
IV. Parameter scans	11
V. Summary	13
Acknowledgments	15
References	15

---

<sup>\*</sup> Corresponding author. [yuzhaoh5@mail.sysu.edu.cn](mailto:yuzhaoh5@mail.sysu.edu.cn)

<sup>†</sup> Corresponding author. [zhh98@mail.sysu.edu.cn](mailto:zhh98@mail.sysu.edu.cn)

## I. INTRODUCTION

Although matter and antimatter are treated symmetrically in particle physics and quantum field theory, stars and galaxies in the celestial neighborhood are constituted exclusively by baryonic matter. Actually, a matter-antimatter symmetric observable universe is excluded by the observation of the cosmic diffuse  $\gamma$ -ray background [1]. The baryon asymmetry of the universe is conventionally quantified by the net baryon-to-photon number density  $\eta_B = (n_B - n_{\bar{B}})/n_\gamma$ . Combining the observations of the cosmic microwave background by the Planck collaboration [2] and the primordial abundances of light elements related to big bang nucleosynthesis,  $\eta_B$  is determined to be [3]

$$\eta_B = (6.13 \pm 0.04) \times 10^{-10}. \quad (1)$$

In order to generate such a baryon asymmetry, the related physical processes must satisfy three Sakharov conditions [4], i.e., the violation of the baryon number  $B$ , the  $C$  and  $CP$  violations, and the departure from thermal equilibrium. The standard model (SM) by itself could fulfill all the three conditions. The  $B$  violation occurs through a nonperturbative effect in electroweak interactions known as the sphaleron processes [5, 6], and the interactions out of thermal equilibrium may happen in a strong first-order electroweak phase transition. This makes electroweak baryogenesis [7] a promising mechanism to generate the baryon asymmetry. However, subsequent researches reveal that the electroweak phase transition in the SM is just a smooth crossover because the Higgs boson mass is too large [8–10]. Thus, a successful baryogenesis can only take place in new physics beyond the SM. Some comprehensive reviews can be found in Refs. [11–13].

Among new physics theories trying to explain the origin of the baryon asymmetry, leptogenesis [14, 15] is a well-motivated mechanism related to the tiny masses of active neutrinos. It typically introduces three generations of heavy right-handed neutrinos (RHNs), allowing active neutrinos to acquire Majorana masses through the type-I seesaw mechanism [16–18]. The decays of RHNs give rise to the lepton asymmetry, which is subsequently converted into the baryon asymmetry via the sphaleron processes. Such a leptogenesis mechanism can be realized in various models (see Refs. [19–35] for an incomplete list of recent works).

Nevertheless, the standard thermal leptogenesis typically requires a high mass scale of the RHNs. For achieving an adequate  $CP$  violation in RHN decays, the lightest RHN mass should be larger than  $10^9$  GeV [36]. Moreover, the generated lepton asymmetry would be strongly washed out if the RHN Yukawa couplings are too large [37–39]. Taking into account the washout effect and the neutrino oscillation data, it demands the lightest RHN mass to be at least  $\sim 10^{10}$  GeV for obtaining the correct baryon-to-photon ratio [37]. Such a high mass scale is challenging to be further tested by experiments.

In order to circumvent a strong washout effect and/or lower down the RHN mass scale, several solutions were proposed. One solution is to assume leptogenesis originating from the reheating process after inflation [40–42]. Another approach is to reprocess  $CP$ -violating interactions at

high scales into the  $B - L$  asymmetry by RHN interactions at lower scales, known as wash-in leptogenesis [43, 44]. Additional avenues include considering nonthermal particle production from the evaporation of primordial black holes [45–49], imposing restrictions on the related couplings [50, 51], embedding leptogenesis within a first-order phase transition [52], and assuming nonstandard cosmology [53, 54]. Besides, a lower RHN mass scale can also be achieved by resonant leptogenesis [55–60], flavored leptogenesis [61–63], and extra  $CP$ -violation by an additional scalar [64].

Motivated by these efforts, we propose another approach to decrease the RHN mass scale by introducing a scalar boson  $\phi$  that decays into RHNs after the  $\phi$  particles are out of thermal equilibrium<sup>1</sup>. We assume a slow decay rate of  $\phi$  to ensure the continuous production of RHNs, even when the washout processes are suppressed at low temperatures. Thus, it provides an additional nonthermal source for the lepton asymmetry. By tracking the particle number density evolution in this scenario, we will explore the suitable parameter regions that can effectively lower down the lightest RHN mass.

The paper is structured as follows. In Section II, we introduce our model, which extends the SM by incorporating a scalar field and three RHNs, and outline the calculations of the  $CP$  asymmetry and the requisite decay widths and scattering cross sections. Section III is dedicated to analyzing the Boltzmann equations and number densities to assess the efficacy of the model. In Section IV, we explore the viable parameter regions by performing parameter scans. Finally, we conclude this work in Section V.

## II. MODEL

We extend the SM with three generations of RHNs  $N_{iR}$  ( $i = 1, 2, 3$ ) and a real scalar  $\phi$ , which is an SM gauge singlet. The  $CP$ -violating decays of the RHNs are expected to give rise to an asymmetry in the lepton number  $L$ . The related Lagrangian is

$$\begin{aligned}
 -\mathcal{L} \supset & \left( h_{\nu,ij} \overline{L_{iL}} \tilde{H} N_{jR} + \frac{1}{2} M_{N_i} \overline{N_{iR}^c} N_{iR} + \frac{1}{2} y_i \overline{N_{iR}^c} N_{iR} \phi + \text{H.c.} \right) \\
 & + m_\phi^2 \phi^2 + \kappa H^\dagger H \phi + \lambda_{\phi H} H^\dagger H \phi^2.
 \end{aligned} \tag{2}$$

Here  $L_{iL}$  represent the  $SU(2)_L$  doublets of the left-handed leptons, and  $\tilde{H} = i\sigma_2 H^*$  is the iso-doublet of the SM Higgs field

$$H = \begin{pmatrix} H^+ \\ H^0 \end{pmatrix}, \tag{3}$$

which develops a vacuum expectation value  $v = 174$  GeV, leading to the spontaneous breaking of the electroweak gauge symmetry.  $N_{iR}$  carry no  $U(1)_Y$  charges and weakly couple to the real scalar  $\phi$  via the Yukawa couplings  $y_i$ .  $N_{iR}^c$  are the charge conjugates of  $N_{iR}$ . The Yukawa couplings  $h_{\nu,ij}$  give Dirac mass terms for the neutrinos after electroweak symmetry breaking,

<sup>1</sup> The impact of a scalar coupling to RHNs has also been studied in Refs. [65, 66] for other motivations.

while  $M_{N_i}$  provide Majorana mass terms. Among the couplings between  $\phi$  and the SM Higgs doublet  $H$ ,  $\kappa$  is a dimension-1 coupling constant, while  $\lambda_{\phi H}$  is dimensionless. We assume that  $\phi$  does not develop a nonzero vacuum expectation value and its mass is just given by  $m_\phi$ .

After the electroweak symmetry breaking, the mass terms for the neutrinos become

$$-\mathcal{L}_{\text{mass}} = \frac{1}{2} \begin{pmatrix} \bar{\nu}_L & \bar{N}_R^c \end{pmatrix} \begin{pmatrix} 0 & v h_\nu \\ v h_\nu^T & M \end{pmatrix} \begin{pmatrix} \nu_L^c \\ N_R \end{pmatrix}, \quad (4)$$

where  $M = \text{diag}(M_{N_1}, M_{N_2}, M_{N_3})$  is the diagonal mass matrix for RHNs. Through a block-diagonalization of the  $6 \times 6$  mass matrix in  $\mathcal{L}_{\text{mass}}$ , the  $3 \times 3$  mass matrix for the active neutrinos is given by

$$M_\nu \simeq -v^2 h_\nu M^{-1} h_\nu^T \quad (5)$$

for  $M \gg v h_\nu$ . Thus, the large RHN masses give an origin to the tiny masses of the active neutrinos via the type-I seesaw mechanism. On the other hand, the flavor eigenstates of the RHNs basically coincide with their mass eigenstates, and three Majorana spinor fields can be constructed by  $N_i = N_{iR}^c + N_{iR}$ . The masses of the corresponding heavy Majorana neutrinos  $N_i$  are approximately given by  $M_{N_i}$ .

A specific form of the Yukawa coupling matrix  $h_\nu$  can be derived by the Casas-Ibarra parametrization [67]. The active neutrino mass matrix  $M_\nu$ , which is complex and symmetric, can be diagonalized by the unitary Pontecorvo–Maki–Nakagawa–Sakata (PMNS) matrix  $U$  [68, 69]:

$$U^T M_\nu U = M_\nu^d, \quad (6)$$

where  $M_\nu^d = \text{diag}(m_1, m_2, m_3)$ . Blending Eqs. (5) and (6), we have

$$-v^2 U^T h_\nu M^{-1} h_\nu^T U = M_\nu^d, \quad (7)$$

and it is not difficult to obtain

$$-v^2 \left[ \left( \sqrt{M_\nu^d} \right)^{-1} U^T h_\nu \left( \sqrt{M} \right)^{-1} \right] \left[ \left( \sqrt{M} \right)^{-1} h_\nu^T U \left( \sqrt{M_\nu^d} \right)^{-1} \right] = I_{3 \times 3}, \quad (8)$$

where the square root of a diagonal matrix means the square roots of its diagonal elements. Thus,

$$R^T \equiv -i v \left( \sqrt{M_\nu^d} \right)^{-1} U^T h_\nu \left( \sqrt{M} \right)^{-1} \quad (9)$$

must be a  $3 \times 3$  complex orthogonal matrix satisfying  $R^T R = I_{3 \times 3}$ . Therefore, the Yukawa coupling matrix can be expressed as

$$h_\nu = \frac{i}{v} U^* \sqrt{M_\nu^d} R^T \sqrt{M}, \quad (10)$$

TABLE I. Three-flavor global fit results of neutrino oscillation parameters in  $1\sigma$  range.

$\theta_{12}$ ( $^\circ$ )	$\theta_{23}$ ( $^\circ$ )	$\theta_{13}$ ( $^\circ$ )	$\delta_{CP}$ ( $^\circ$ )	$\Delta m_{21}^2$ ( $10^{-5}$ eV $^2$ )	$\Delta m_{31}^2$ ( $10^{-3}$ eV $^2$ )
$33.44^{+0.77}_{-0.74}$	$49.2^{+1.0}_{-1.3}$	$8.57^{+0.13}_{-0.12}$	$194^{+52}_{-25}$	$7.42^{+0.21}_{-0.20}$	$2.515^{+0.028}_{-0.028}$

which implies that larger values in the RHN mass matrix  $M$  leads to larger Yukawa couplings  $h_\nu$  if the other parameters are fixed.

Following Particle Data Group's convention [70] for the parametrization of the PMNS matrix, we have

$$U = \begin{pmatrix} c_{12}c_{13} & s_{12}c_{13} & s_{13}e^{-i\delta_{CP}} \\ -s_{12}c_{23} - c_{12}s_{13}s_{23}e^{i\delta_{CP}} & c_{12}c_{23} - s_{12}s_{13}s_{23}e^{i\delta_{CP}} & c_{13}s_{23} \\ s_{12}s_{23} - c_{12}s_{13}c_{23}e^{i\delta_{CP}} & -c_{12}s_{23} - s_{12}s_{13}c_{23}e^{i\delta_{CP}} & c_{13}c_{23} \end{pmatrix} \begin{pmatrix} e^{i\eta_1} & 0 & 0 \\ 0 & e^{i\eta_2} & 0 \\ 0 & 0 & 1 \end{pmatrix}, \quad (11)$$

where  $c_{ij} \equiv \cos \theta_{ij}$ ,  $s_{ij} \equiv \sin \theta_{ij}$ .  $\delta_{CP}$  is the Dirac  $CP$  phase and  $\eta_{1,2}$  are the Majorana  $CP$  phases. In the following calculation, we assume a normal hierarchy for the active neutrino masses, and set the Majorana phases to be zero and the neutrino oscillation parameters to be the best fit values from the global analysis given by the NuFIT collaboration [71], which are listed in Table I.

Moreover, we assume the lightest neutrino mass  $m_1$  to be zero, leading to  $m_2 = \sqrt{\Delta m_{21}^2}$  and  $m_3 = \sqrt{\Delta m_{31}^2}$ . In this case, the complex orthogonal matrix  $R$  can be described by a single complex parameter  $z = z_r + iz_i$  [72] with a form of

$$R = \begin{pmatrix} 0 & \cos z & \sin z \\ 0 & -\sin z & \cos z \\ 1 & 0 & 0 \end{pmatrix}. \quad (12)$$

for the normal hierarchy. Thus, given the values of  $m_{N_1}$ ,  $m_{N_2}$ ,  $m_{N_3}$ ,  $z_r$ , and  $z_i$ , the Yukawa coupling matrix  $h_\nu$  can be determined through Eq. (10).

The  $CP$  asymmetry in the decays of the heavy Majorana neutrino  $N_i$  to light leptons and Higgs bosons can be measured by

$$\varepsilon_i = \frac{\Gamma(N_i \rightarrow \ell H) - \Gamma(N_i \rightarrow \bar{\ell} \bar{H})}{\Gamma(N_i \rightarrow \ell H) + \Gamma(N_i \rightarrow \bar{\ell} \bar{H})}, \quad (13)$$

where  $\ell = \ell_j^-, \nu_j$  ( $j = 1, 2, 3$ ) and  $H = H^+, H^0$ , while  $\bar{\ell}$  and  $\bar{H}$  represent their antiparticles. Considering the interference of one-loop diagrams with tree-level diagrams, it is given by [73]

$$\varepsilon_i = \frac{1}{8\pi} \sum_{j \neq i} \left[ f \left( \frac{M_{N_j}^2}{M_{N_i}^2} \right) - \frac{M_{N_i} M_{N_j}}{M_{N_j}^2 - M_{N_i}^2} \right] \frac{\text{Im}\{[(h_\nu^\dagger h_\nu)_{ij}]^2\}}{(h_\nu^\dagger h_\nu)_{ii}}, \quad (14)$$

where  $f(x) = \sqrt{x}\{1 - (1+x)\ln[(1+x)/x]\}$ . Basically,  $\varepsilon_i$  are positively correlated to the Yukawa couplings  $h_{\nu,ij}$ , which are positively correlated to  $M_{N_i}$  as mentioned above. When the

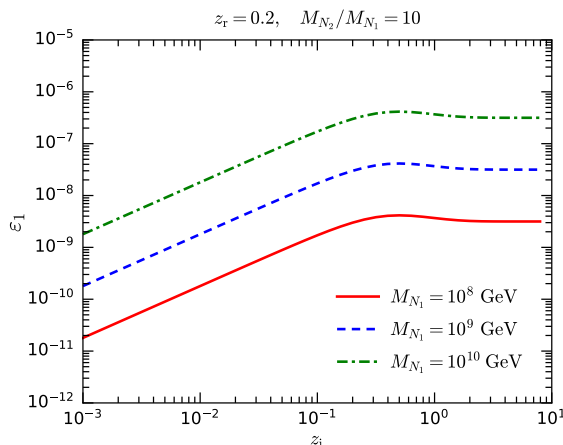


FIG. 1. The  $CP$  asymmetry  $\varepsilon_1$  as functions of  $z_i$  for  $M_{N_1} = 10^8, 10^9$ , and  $10^{10}$  GeV with  $z_r = 0.2$ ,  $M_{N_2} = 10M_{N_1}$ , and  $M_{N_3} \rightarrow \infty$ .

$CP$ -violating  $N_i$  decays are out of thermal equilibrium, a lepton number asymmetry would be generated.

In Fig. 1, we demonstrate the  $CP$  asymmetry in the  $N_1$  decays as functions of  $z_i$  for  $M_{N_1} = 10^8, 10^9$ , and  $10^{10}$  GeV. The other parameters are fixed as  $z_r = 0.2$ ,  $M_{N_2} = 10M_{N_1}$ , and  $M_{N_3} \rightarrow \infty$ . It is evident that the  $CP$  asymmetry  $\varepsilon_1$  is basically proportional to  $M_{N_1}$ . Moreover,  $\varepsilon_1$  increases as  $z_i$  increases for  $z_i \lesssim 0.4$ , but it tends to be saturated for  $z_i \gtrsim 0.4$ .

For simplicity, we further assume a mass hierarchy of the heavy Majorana neutrinos as  $M_{N_1} \ll M_{N_2}, M_{N_3}$ . As a result, the lepton asymmetry generated by  $N_2$  and  $N_3$  will be washed out by the inverse decay processes  $\ell H/\bar{\ell}\bar{H} \rightarrow N_1$ . Therefore, only the  $B-L$  numbers yielded from  $N_1$  remain and are subsequently converted into the baryon asymmetry through the electroweak sphaleron processes [6]. This is the one-flavor approximation. After the electroweak crossover, the sphaleron processes freeze out, and the resulting baryon-to-photon ratio at recombination can be estimated as [12]

$$\eta_B = \frac{c_s}{f} \frac{n_{B-L}}{n_\gamma} \simeq 0.013 \frac{n_{B-L}}{n_\gamma}. \quad (15)$$

Here,  $n_{B-L}$  and  $n_\gamma$  represent the number densities of the  $B-L$  charges and the photons, respectively.  $c_s = 28/79$  is the conversion ratio of the  $B-L$  asymmetry to the baryon asymmetry via the sphaleron processes for the inclusion of three RHNs [74].  $f = 2387/86$  is a dilution factor accounting for the increase in  $n_\gamma$  in a comoving volume from the epoch with  $T \sim m_{N_1}$  to recombination.

The washout effect plays a crucial role in diminishing the final yield of  $n_{B-L}$ . The primary washout processes are the inverse decays  $\ell H/\bar{\ell}\bar{H} \rightarrow N_1$ . They are related to the decay width of  $N_1$ , which is given by

$$\Gamma_{N_1} = \Gamma(N_1 \rightarrow \ell H) + \Gamma(N_1 \rightarrow \bar{\ell}\bar{H}) \simeq \frac{1}{8\pi} (h_\nu^\dagger h_\nu)_{11} M_{N_1}, \quad (16)$$

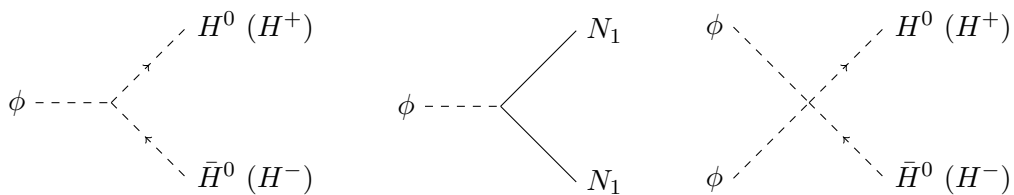


FIG. 2. Decay and scattering diagrams for the scalar  $\phi$ .

where the masses of light leptons and Higgs bosons have been neglected.

In our scenario extending the standard leptogenesis, the additional real scalar  $\phi$  could decay into RHNs. For simplicity, we assume a mass hierarchy of

$$2M_{N_1} < m_\phi < 2M_{N_2} \ll M_{N_3}, \quad (17)$$

which implies that  $\phi$  can only decay into  $N_1 N_1$  and  $H \bar{H}$ . The relevant decay and annihilation diagrams for  $\phi$  are illustrated in Fig. 2. At tree level, the partial decay widths for  $\phi \rightarrow N_1 N_1$  and  $\phi \rightarrow H \bar{H}$  are

$$\Gamma(\phi \rightarrow N_1 N_1) = \frac{y_1^2 m_\phi}{16\pi} \left(1 - \frac{4M_{N_1}^2}{m_\phi^2}\right)^{3/2}, \quad (18)$$

$$\Gamma(\phi \rightarrow H \bar{H}) \simeq \frac{\kappa^2}{8\pi m_\phi}. \quad (19)$$

The annihilation cross sections for  $\phi\phi \rightarrow H \bar{H}$  are given by

$$\sigma(\phi\phi \rightarrow H^0 \bar{H}^0) = \sigma(\phi\phi \rightarrow H^+ H^-) \simeq \frac{\lambda_{\phi H}^2}{4\pi s \sqrt{1 - 4m_\phi^2/s}}, \quad (20)$$

where  $s$  is a Mandelstam variable.

The  $\phi$  decays into  $N_1 N_1$  are followed by the subsequent  $N_1$  decays, which give rise to the lepton asymmetry if the  $N_1$  particles depart from thermal equilibrium. If the  $\phi$  lifetime is sufficiently long, the production of  $N_1$  particles persists even when the washout effect is suppressed at low temperatures. In the next section, we will provide a comprehensive analysis for the evolution of the lepton asymmetry.

### III. BOLTZMANN EQUATIONS

In this section, we utilize a set of Boltzmann equations [12, 75, 76] to study the evolution of the number densities of the  $\phi$  particles, the  $N_1$  particles, and the  $B - L$  charges, which are denoted by  $n_\phi$ ,  $n_{N_1}$ , and  $n_{B-L}$ , respectively. With the assumptions made in the previous section,

the Boltzmann equation for  $n_\phi$  reads

$$\begin{aligned} \frac{dn_\phi}{dt} + 3Hn_\phi = & -\langle\Gamma_{\phi\rightarrow N_1N_1}\rangle \left[ n_\phi - \frac{n_\phi^{\text{eq}}n_{N_1}^2}{(n_{N_1}^{\text{eq}})^2} \right] - \langle\Gamma_{\phi\rightarrow H\bar{H}}\rangle (n_\phi - n_\phi^{\text{eq}}) \\ & - \langle\sigma_{\phi\phi\rightarrow H\bar{H}}v\rangle \left[ n_\phi^2 - (n_\phi^{\text{eq}})^2 \right], \end{aligned} \quad (21)$$

where  $H$  is the Hubble expansion rate, and the collision terms are related to the  $\phi \leftrightarrow N_1N_1$ ,  $\phi \leftrightarrow H\bar{H}$ , and  $\phi\phi \leftrightarrow H\bar{H}$  processes.  $n_i^{\text{eq}}$  indicate the number densities in thermal equilibrium, while  $\langle\Gamma_i\rangle$  and  $\langle\sigma_{\phi\phi\rightarrow H\bar{H}}v\rangle$  denote the thermal averages of the decay width  $\Gamma_i$  and the  $\phi\phi \rightarrow H\bar{H}$  scattering cross section  $\sigma_{\phi\phi\rightarrow H\bar{H}}$  multiplied by the Møller velocity, respectively.

Taking into account the  $N_1 \leftrightarrow \ell H/\bar{\ell}\bar{H}$  and  $\phi \leftrightarrow N_1N_1$  processes, the Boltzmann equation for  $n_{N_1}$  is

$$\frac{dn_{N_1}}{dt} + 3Hn_{N_1} = -\langle\Gamma_{N_1}\rangle (n_{N_1} - n_{N_1}^{\text{eq}}) + \langle\Gamma_{\phi\rightarrow N_1N_1}\rangle \left[ n_\phi - \frac{n_\phi^{\text{eq}}n_{N_1}^2}{(n_{N_1}^{\text{eq}})^2} \right]. \quad (22)$$

Moreover, the evolution of  $n_{B-L}$  is governed by

$$\frac{dn_{B-L}}{dt} + 3Hn_{B-L} = -\varepsilon_1\langle\Gamma_{N_1}\rangle (n_{N_1} - n_{N_1}^{\text{eq}}) - \frac{1}{2}\langle\Gamma_{N_1}\rangle \frac{n_{N_1}^{\text{eq}}n_{B-L}}{n_\ell^{\text{eq}}}, \quad (23)$$

where the first term in the right-hand side corresponds to the generation of the lepton asymmetry by the  $CP$  asymmetry  $\varepsilon_1$  and the departure of the  $N_1$  particles from thermal equilibrium, and the second term, which is proportional to  $n_{B-L}$ , indicates the washout of the generated lepton asymmetry caused by the inverse decays.

In order to separate the dynamical evolution from the cosmological expansion effect, it is more convenient to use the ratios of these number density to the photon number density,  $Y_i = n_i/n_\gamma$ . A dimensionless parameter  $x = M_{N_1}/T$  is further introduced to replace the temperature  $T$ . Thus, the set of Boltzmann equations can be transformed into a simplified form,

$$\begin{aligned} \frac{dY_\phi}{dx} = & -\frac{x\langle\Gamma_{\phi\rightarrow N_1N_1}\rangle}{H(M_{N_1})} \left[ Y_\phi - \frac{Y_\phi^{\text{eq}}Y_{N_1}^2}{(Y_{N_1}^{\text{eq}})^2} \right] - \frac{x\langle\Gamma_{\phi\rightarrow H\bar{H}}\rangle}{H(M_{N_1})} (Y_\phi - Y_\phi^{\text{eq}}) \\ & - \frac{xn_\gamma\langle\sigma_{\phi\phi\rightarrow H\bar{H}}v\rangle}{H(M_{N_1})} \left[ Y_\phi^2 - (Y_\phi^{\text{eq}})^2 \right], \end{aligned} \quad (24)$$

$$\frac{dY_{N_1}}{dx} = -\frac{x\langle\Gamma_{N_1}\rangle}{H(M_{N_1})} (Y_{N_1} - Y_{N_1}^{\text{eq}}) + \frac{x\langle\Gamma_{\phi\rightarrow N_1N_1}\rangle}{H(M_{N_1})} \left[ Y_\phi - \frac{Y_\phi^{\text{eq}}Y_{N_1}^2}{(Y_{N_1}^{\text{eq}})^2} \right], \quad (25)$$

$$\frac{dY_{B-L}}{dx} = -\frac{x\varepsilon_1\langle\Gamma_{N_1}\rangle}{H(M_{N_1})} (Y_{N_1} - Y_{N_1}^{\text{eq}}) - \frac{x\langle\Gamma_{N_1}\rangle Y_{N_1}^{\text{eq}}}{2H(M_{N_1})Y_\ell^{\text{eq}}} Y_{B-L}, \quad (26)$$

where  $Y_i^{\text{eq}} \equiv n_i^{\text{eq}}/n_\gamma$  and  $H(M_{N_1})$  is the Hubble rate at  $T = M_{N_1}$ .

Furthermore,  $\langle\Gamma_i\rangle$  can be expressed as [77, 78]

$$\langle\Gamma_i\rangle = \frac{K_1(x)}{K_2(x)} \Gamma_i, \quad (27)$$

TABLE II. Information for two BPs.

	$M_{N_1}$ (GeV)	$M_{N_2}$ (GeV)	$z_r$	$z_i$	$m_\phi$	$y_1$	$\kappa$ (GeV)	$\lambda_{\phi H}$
BP I	$10^{10}$	$10^{11}$	0.2	3	$2.5M_{N_1}$	$1.11 \times 10^{-4}$	100	$10^{-4}$
BP II	$2 \times 10^9$	$2 \times 10^{10}$	0.2	0.2	$2.5M_{N_1}$	$4.6 \times 10^{-5}$	100	$10^{-4}$

TABLE III. Values of  $h_\nu$ ,  $\varepsilon_1$ , and  $\Gamma_{N_1}$  for two BPs.

	$h_\nu$	$\varepsilon_1$	$\Gamma_{N_1}$ (GeV)
BP I	$\begin{pmatrix} 0.42 + 0.54i & -1.72 + 1.31i & 0.01 \\ 1.60 - 2.84i & 9.03 + 5.04i & 0 \\ -0.45 - 2.82i & 8.97 - 1.41i & 0 \end{pmatrix} \times 10^{-2}$	$3.17 \times 10^{-7}$	$7.67 \times 10^5$
BP II	$\begin{pmatrix} 0.33 + 0.02i & -0.87 - 0.34i & 0.15 \\ 0.72 - 0.28i & 4.01 + 0.47i & -0.05 - 0.01i \\ -0.21 - 0.28i & 4.00 - 0.11i & 0.09 - 0.01i \end{pmatrix} \times 10^{-3}$	$5.99 \times 10^{-8}$	66.04

where  $K_j(x)$  represents the the second kind modified Bessel function of order  $j$ .  $\langle \sigma_{\phi\phi \rightarrow H\bar{H}} v \rangle$  can be calculated by [79, 80]

$$\langle \sigma_{\phi\phi \rightarrow H\bar{H}} v \rangle = \frac{T}{32\pi^4 (n_\phi^{\text{eq}})^2} \int_{4m_\phi^2}^{\infty} ds \sqrt{s} (s - 4m_\phi^2) \sigma_{\phi\phi \rightarrow H\bar{H}}(s) K_1\left(\frac{\sqrt{s}}{T}\right). \quad (28)$$

The washout effect in Eq. (26) is related to a factor of [78]

$$W_{\text{ID}}(x) = \frac{x \langle \Gamma_{N_1} \rangle}{2H(M_{N_1})} \frac{Y_{N_1}^{\text{eq}}}{Y_\ell^{\text{eq}}} = \frac{x^3 K_1(x) \Gamma_N}{4H(M_{N_1})}. \quad (29)$$

Below we solve the set of Boltzmann equations by numerical methods. We assume that after reheating, the  $\phi$  particles and all SM particles are in thermal equilibrium, while there are no  $N_i$  particles because their interactions are too weak. Thus, the initial conditions can be set as  $Y_\phi = Y_\phi^{\text{eq}}$  and  $Y_{N_1} = Y_{B-L} = 0$  at  $x = 0.1$ . We choose two benchmark points (BPs) for the model parameters, as outlined in the Table II. The Yukawa coupling matrix  $h_\nu$  is determined by the Casas-Ibarra parametrization. We present the values of the  $h_\nu$  elements, the  $CP$  asymmetry  $\varepsilon_1$ , and the  $N_1$  decay width  $\Gamma_{N_1}$  calculated for the two BPs in Table III. Compared to BP I with  $z_i = 3$ , BP II with  $z_i = 0.2$  has a smaller  $CP$  asymmetry  $\varepsilon_1$  and a much smaller  $\Gamma_{N_1}$ . Thus, the washout effect in BP II is expected to be much weaker than in BP I.

In order to evaluate the impact of the scalar  $\phi$ , we separately demonstrate the evolution of number densities in the standard thermal leptogenesis without  $\phi$  and that in the scalar-assisted leptogenesis. For the strong washout scheme BP I,  $Y_{N_1}$ ,  $|Y_{B-L}|$ , and  $(Y_{N_1} - Y_{N_1}^{\text{eq}})/Y_{N_1}^{\text{eq}}$  as functions of  $x$  in standard case are illustrated in left panel of Fig. 3, while  $Y_\phi$  and  $Y_\phi^{\text{eq}}$  are also plotted in the right panel of Fig. 3 for the scalar-assisted case.

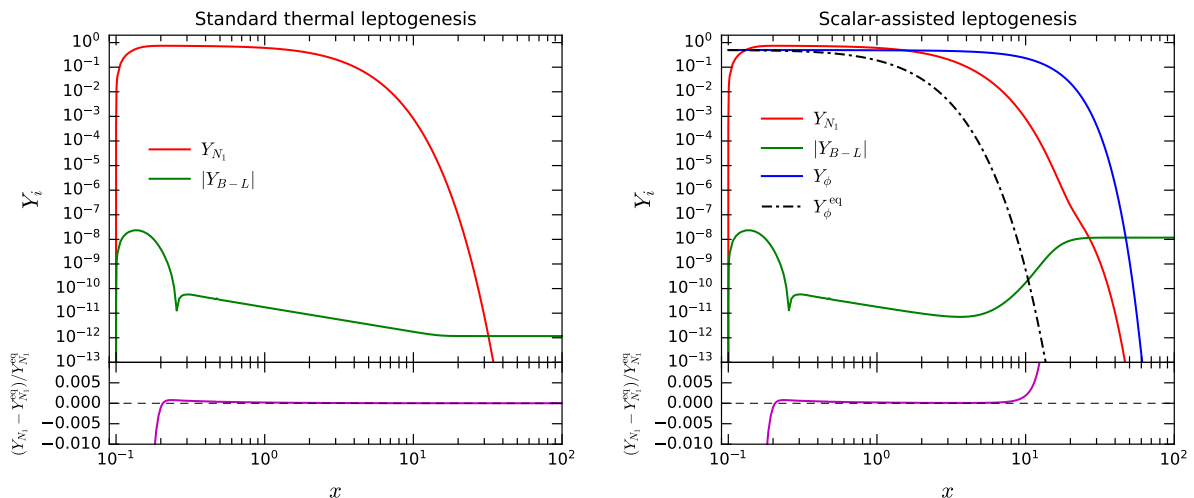


FIG. 3. Evolution of  $Y_{N_1}$ ,  $Y_{B-L}$ ,  $(Y_{N_1} - Y_{N_1}^{\text{eq}})/Y_{N_1}^{\text{eq}}$ ,  $Y_{\phi}$ , and  $Y_{\phi}^{\text{eq}}$  as functions of  $x = M_{N_1}/T$  in the standard (left) and scalar-assisted (right) leptogenesis for BP I, which is a strong washout scheme. The final baryon-to-photon ratios are  $\eta_B = 7.16 \times 10^{-14}$  (left) and  $\eta_B = 6.1 \times 10^{-10}$  (right).

In the standard case of BP I, although we have set a vanishing initial number density for  $N_1$ , the  $N_1$  particles are rapidly thermalized via interactions with the SM plasma, and  $Y_{N_1}$  quickly approaches the thermal value  $Y_{N_1}^{\text{eq}}$ . The  $CP$ -violating  $N_1 \leftrightarrow \ell H/\bar{\ell}\bar{H}$  processes for nonzero  $Y_{N_1} - Y_{N_1}^{\text{eq}}$  generate the lepton asymmetry, leading to the sudden increase of  $|Y_{B-L}|$  from  $x = 0.1$ . Then the washout processes begin to reduce the produced lepton asymmetry, resulting in the decrease of  $|Y_{B-L}|$ . There is a sharp change in the  $|Y_{B-L}|$  curve at  $x \sim 0.25$ , and it corresponds to the sign flip of  $Y_{B-L}$  because the first negative  $Y_{N_1} - Y_{N_1}^{\text{eq}}$  become positive after  $x \sim 0.2$ . For  $x \gtrsim 0.25$ , the net lepton numbers are regenerated under the competition between the generation and washout processes. The  $Y_{B-L}$  value tends to be steady for  $x \gtrsim 20$ , where both the generation and washout of the lepton symmetry are suppressed at such low temperatures. This leads to a final baryon-to-photon ratio of  $\eta_B = 7.16 \times 10^{-14}$ , which is too low to account for the observed value (1).

In the scalar-assisted case of BP I, the  $\phi$  particles become out of thermal equilibrium after  $x \sim 0.3$ , and the  $\phi \rightarrow N_1 N_1$  decays give rise to nonthermal production of  $N_1$  particles. At low temperatures, such an extra source for the  $N_1$  particles helps the generation of the lepton asymmetry. As demonstrated in the right panel of Fig. 3,  $|Y_{B-L}|$  rises again at  $x \sim 4$ , and becomes constant for  $x \gtrsim 30$ , resulting in a final  $\eta_B$  of  $6.1 \times 10^{-10}$  to explain the observation.

Similarly, we present the results for the weak washout scheme BP II in Fig. 4. Compared with BP I, the small  $\Gamma_{N_1}$  in BP II slows down the thermalization of  $N_1$  particles, and  $Y_{N_1}$  becomes close to  $Y_{N_1}^{\text{eq}}$  at  $x \sim 1$ . A small  $\Gamma_{N_1}$  also implies a weak washout effect, and hence the decrease of  $|Y_{B-L}|$  after  $x \gtrsim 2$  is quite slow. In the standard case, the final  $\eta_B$  is  $3.65 \times 10^{-11}$ , lower than the observed value by one order of magnitude. In the scalar-assisted case,  $|Y_{B-L}|$  is lifted after  $x \sim 4$ , leading to a final  $\eta_B$  of  $6.1 \times 10^{-10}$ .

The discussions above show that the introduction of the scalar  $\phi$  can effectively enhance the

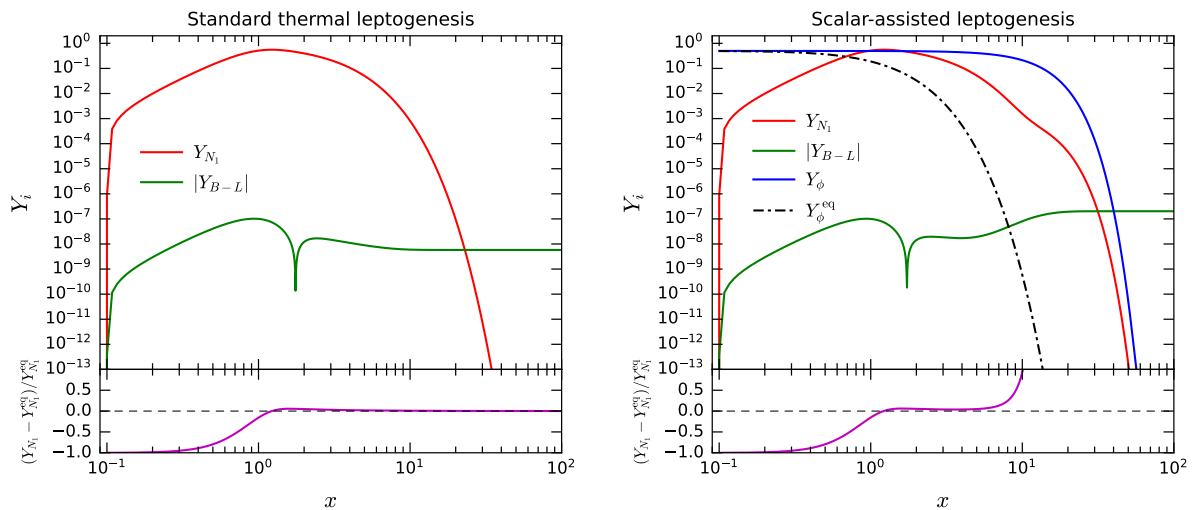


FIG. 4. Same as Fig. 3, but for BP II, which is a weak washout scheme. The final  $\eta_B$  are  $3.65 \times 10^{-11}$  (left) and  $6.1 \times 10^{-10}$  (right).

generation of the lepton asymmetry, especially in a strong washout scheme. Such an enhancement depends on the  $\phi \rightarrow N_1 N_1$  decay width, which is proportional to the square of the Yukawa coupling  $y_1$ . Below, we investigate the impact of  $y_1$  on the resulting baryon-to-photon ratio  $\eta_B$ .

In the left panel of Fig. 5, we show  $\eta_B$  as functions of  $y_1$  for  $z_i = 0.1, 0.5$ , and 1 with  $M_{N_1} = 10^9$  GeV and  $M_{N_2} = 10^{10}$  GeV in the scalar-assisted leptogenesis. The values of the remaining parameters are the same as in BP II. For a fixed  $z_i$ , it is observed that a smaller  $y_1$  leads to a larger  $\eta_B$ , because  $\phi$  particles with a longer lifetime would maintain a high number density for a longer time to produce more  $N_1$  particles. For  $y_1 \gtrsim 2 \times 10^{-4}$ , the lifetime of the  $\phi$  boson is too short to produce extra  $N_1$  particles, and the resulting  $\eta_B$  are basically the same as in the standard leptogenesis. Note that a larger  $z_i$  means a larger washout effect, and the  $z_i = 1$  case would lead to the lowest  $\eta_B$  among the three cases for  $y_1 \gtrsim 2 \times 10^{-4}$ . Nonetheless, for  $y_1 \lesssim 5 \times 10^{-3}$ , the  $\phi$  decays could overcome the strong washout in the  $z_i = 1$  case, making  $\eta_B$  comparable to those in the other cases.

In the right panel of Fig. 5, similar results are presented for  $M_{N_1} = 10^8, 10^9$ , and  $10^{10}$  GeV with  $z_i = 0.4$  and  $M_{N_2} = 10M_{N_1}$ . The final  $\eta_B$  is positively correlated to the RHN masses, because a smaller  $M_{N_1}$  would suppress  $\varepsilon_1$  and hence the generation of the lepton asymmetry. Nevertheless, the  $\phi \rightarrow N_1 N_1$  decays with a sufficiently small  $y_1$  can help lift up  $\eta_B$ . The resulting  $\eta_B$  for  $y_1 = 10^{-5}$  in the  $M_{N_1} = 10^8$  GeV case is comparable to that for  $y_1 = 10^{-3}$  in the  $M_{N_1} = 10^9$  GeV case. Thus, the scalar-assisted leptogenesis could effectively lower down the viable  $M_{N_1}$ .

#### IV. PARAMETER SCANS

In order to understand the impact of the scalar  $\phi$ , we perform some parameter scans in this section. Firstly, we conduct a scan in the  $M_{N_1}$ - $z_i$  plane with other parameters taking the values

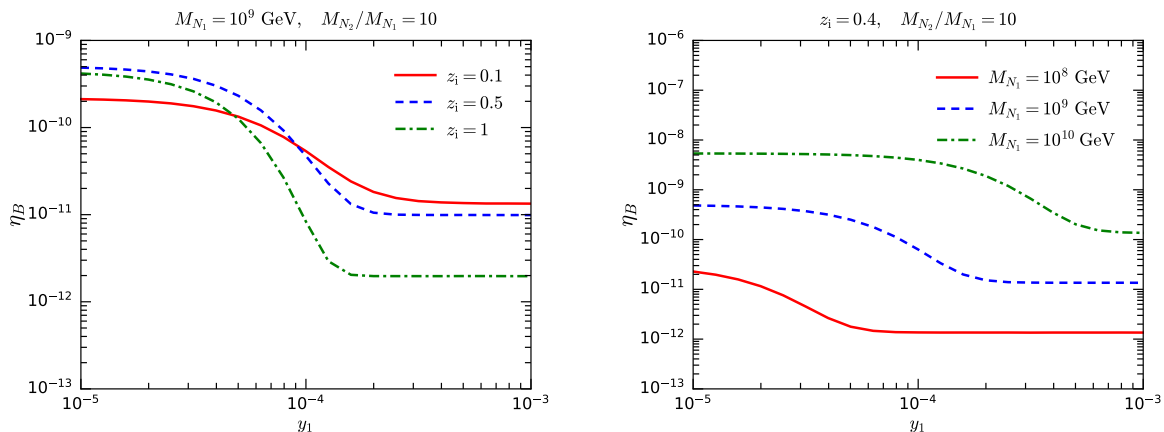


FIG. 5. The baryon-to-photon ratio  $\eta_B$  as functions of the Yukawa coupling  $y_1$  for different values of  $z_i$  with  $M_{N_1} = 10^9$  GeV and  $M_{N_2} = 10^{10}$  GeV (left) and for different values of  $M_{N_1}$  with  $z_i = 0.4$  and  $M_{N_2} = 10M_{N_1}$  (right) in the scalar-assisted leptogenesis. The remaining parameters take the same values in BP II.

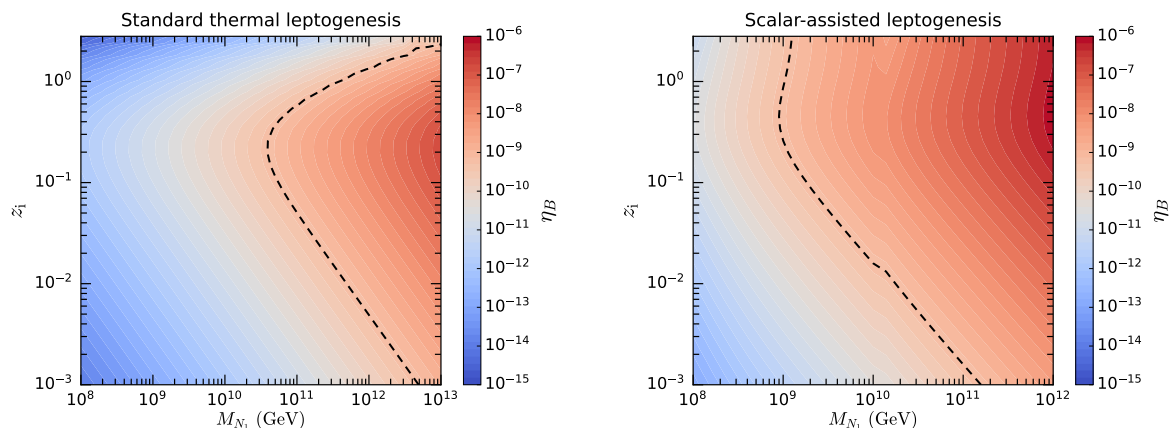


FIG. 6.  $\eta_B$  contours in the  $M_{N_1}$ - $z_i$  plane for the standard (left) and scalar-assisted (right) leptogenesis with the remaining parameters taking the values in BP II. The dashed lines denote the observed value  $\eta_B = 6.13 \times 10^{-10}$ .

in BP II (except for  $M_{N_2} = 10M_{N_1}$ ). Contours of  $\eta_B$  obtained in the standard and scalar-assisted leptogenesis are illustrated in the left and right panels of Fig. 6, respectively.

In both cases, an increase in  $M_{N_1}$  implies an augmentation in the  $CP$  asymmetry  $\varepsilon_1$  that essentially increases  $\eta_B$ . On the other hand, a larger  $z_i$  gives not only a larger  $\varepsilon_1$ , but also a larger  $\Gamma_{N_1}$ , which would enhance the washout effect. Consequently, for a fixed  $M_{N_1}$  in the standard case, the resulting baryon-to-photon ratio increases as  $z_i$  increases from  $10^{-3}$ , and reaches the maximum at  $z_i \sim 0.2$ , and then declines for larger  $z_i$ . In the scalar-assisted case, the nonthermal production of  $N_1$  particles from  $\phi$  decays can significantly increase the resulting  $\eta_B$ . In particular, it compensates the lepton asymmetry diminished by the strong washout for  $z_i \gtrsim 0.2$ . At  $z_i \sim 2$ , the value of  $M_{N_1}$  required for the correct  $\eta_B$  can be reduced by nearly four orders of magnitude, compared to the standard case.

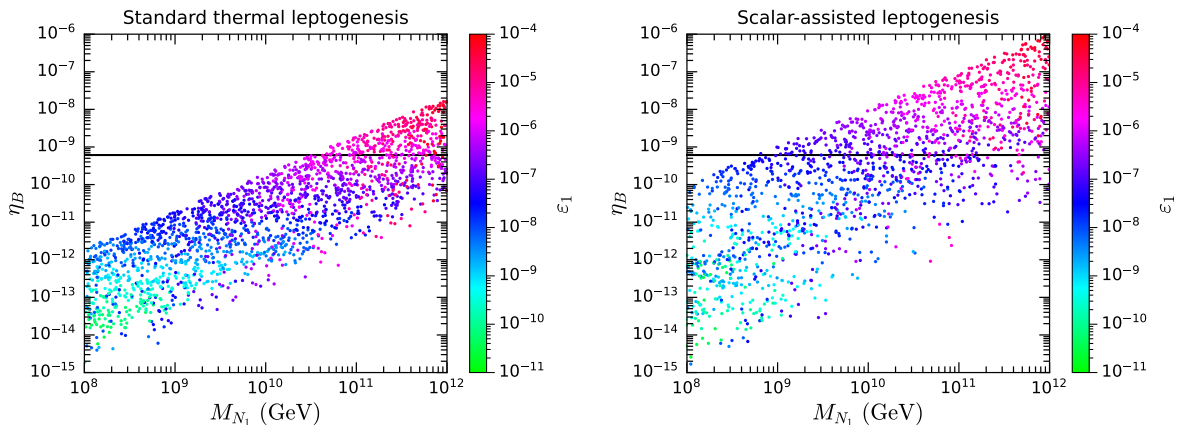


FIG. 7. Parameter points projected into the  $M_{N_1}$ - $\eta_B$  plane for the standard (left) and scalar-assisted (right) leptogenesis. The color axes denote the  $CP$  asymmetry  $\epsilon_1$ , and the black horizontal lines indicate the observed value of the baryon-to-photon ratio.

Furthermore, we carry out a random scan within the following parameter ranges:

$$10^8 \text{ GeV} < M_{N_1} < 10^{12} \text{ GeV}, \quad 3 < M_{N_2}/M_{N_1} < 10^3, \quad 2.01 < m_\phi/M_{N_1} < 10 \quad (30)$$

$$10^{-3} < z_i < 3, \quad 0 < z_r < \pi/4, \quad 10^{-5} < y_1 < 10^{-3}, \quad (31)$$

$$10^{-3} \text{ GeV} < \kappa < 10^2 \text{ GeV}, \quad 10^{-6} \text{ GeV} < \lambda_{\phi H} < 10^{-3} \text{ GeV}. \quad (32)$$

In Fig. 7, we project the parameter points into the  $M_{N_1}$ - $\eta_B$  plane with colors indicating the  $CP$  asymmetry  $\epsilon_1$ . It clearly shows that  $\eta_B$  is positively correlated to both  $M_{N_1}$  and  $\epsilon_1$ . In the standard leptogenesis, the observed baryon-to-photon ratio, which is denoted by the horizontal line, can be achieved for  $M_{N_1} \gtrsim 3 \times 10^{10}$  GeV. On the other hand, as the scalar-assisted leptogenesis provides an extra nonthermal source for  $N_1$  particles, the applicable value of  $M_{N_1}$  can be lowered down to  $\sim 6 \times 10^8$  GeV for the correct  $\eta_B$ . Besides, the required values of  $\epsilon_1$  in the scalar-assisted case are smaller than the standard case.

In order to demonstrate the viable parameter ranges, we pick out the parameter points that lead to a baryon-to-photon ratio  $\eta_B$  within the  $3\sigma$  range of the observational value (1). These parameter points are projected into the  $M_{N_1}$ - $z_i$  and  $M_{N_1}$ - $\epsilon_1$  planes, as illustrated in the left and right panels of Fig. 8, respectively. We find that the introduction of the scalar  $\phi$  significantly enlarges the available parameter regions. Compared to the standard leptogenesis, the applicable  $M_{N_1}$  for the same  $z_i$  can be lowered down by two to four orders of magnitude. The lowest viable  $M_{N_1}$  is reduced from  $\sim 3 \times 10^{10}$  GeV to  $\sim 6 \times 10^8$  GeV, while the smallest viable  $\epsilon_1$  decreases from  $\sim 6 \times 10^{-7}$  to  $\sim 4 \times 10^{-8}$ .

## V. SUMMARY

In order to achieve the observed baryon asymmetry, the mass scale of RHNs in the standard leptogenesis should be rather high to provide a sufficient  $CP$  violation and to overcome the

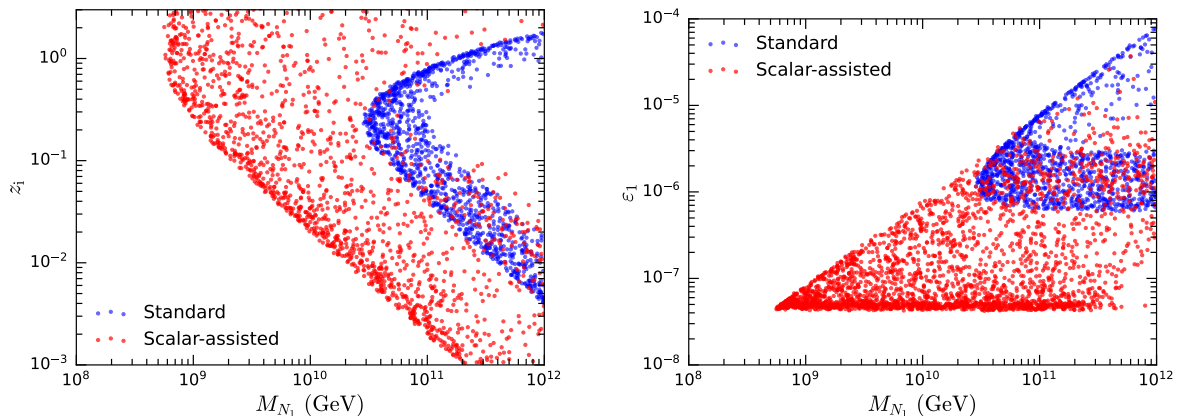


FIG. 8. Selected parameter points with the correct baryon-to-photon ratio projected into the  $M_{N_1}$ - $z_i$  (left) and  $M_{N_1}$ - $\varepsilon_1$  (right) planes. The red and blue dots correspond to the standard and scalar-assisted leptogenesis, respectively.

washout effect. In this work, we have proposed a particular scenario to lower down the RHN mass scale by introducing a scalar  $\phi$  decaying into RHNs because of its Yukawa couplings.  $\phi$  particles should have an adequate long lifetime so that their decays provide an additional nonthermal source for the RHNs after the washout effect is attenuated. Therefore, such a scalar-assisted leptogenesis can improve the generation of the lepton asymmetry, and the required RHN mass scale would be lower than the standard case.

To investigate the efficiency of our proposal, we have conducted a detailed analysis based on the one-flavor approximation, where only the  $N_1 \leftrightarrow \ell H/\bar{\ell}\bar{H}$  processes are relevant to the generation of the lepton asymmetry. A set of Boltzmann equations describing the evolution of the related number densities are established and solved. The number densities as functions of  $x = M_{N_1}/T$  are demonstrated for two BPs. For BP I with a strong washout effect, we have found that the inclusion of the scalar  $\phi$  can lift up the final baryon-to-photon ratio  $\eta_B$  by four orders of magnitude, compared to the standard leptogenesis. For BP II with a weak washout effect,  $\eta_B$  can be increased by one order of magnitude in the scalar-assisted leptogenesis.

Furthermore, we have carried out parameter scans to explore the parameter space. A scan in the  $M_{N_1}$ - $z_i$  plane with other parameters fixed shows that the resulting baryon asymmetry is widely increased in the scalar-assisted leptogenesis, especially in the parameter regions where the washout effect is strong. At  $z_i \sim 2$ , which leads to a very strong washout, the lightest RHN mass  $M_{N_1}$  required for the observed  $\eta_B$  can be lowered down by nearly four orders of magnitude. Based on a random scan in the parameter space, we have demonstrated the positive correlations of  $\eta_B$  to  $M_{N_1}$  and  $\varepsilon_1$ , and that both the viable  $M_{N_1}$  and  $\varepsilon_1$  in the scalar-assisted case are smaller than those in the standard case. Moreover, from the parameter points that are consistent with the observed baryon-to-photon ratio in the  $3\sigma$  range, we have found that the scalar-assisted leptogenesis can effectively extend the available parameter ranges, lowering down the viable  $M_{N_1}$  by two to four orders of magnitude for the same  $z_i$ .

These results clearly show that the scalar-assisted leptogenesis is a feasible avenue to lower

down the RHN mass scale, particularly when the washout effect is strong. A lower mass scale may more easily be related to rich phenomena that can be tested in experiments. Potential implications of our work may extend beyond the specific model investigated here, offering valuable insights into the leptogenesis mechanism in diverse theoretical frameworks. Since there are a lot of extra scalar fields in new physics beyond the SM, the origin of the scalar  $\phi$  could be linked to other interesting topics, such as the origin of dark matter, grand unification, supersymmetry, and so on.

### ACKNOWLEDGMENTS

This work is supported by the National Natural Science Foundation of China (NSFC) under Grants No. 12275367 and No. 11875327, the Fundamental Research Funds for the Central Universities, the Guangzhou Science and Technology Planning Project under Grants No. 2024A04J4026, and the Sun Yat-Sen University Science Foundation.

- 
- [1] A. G. Cohen, A. De Rujula, and S. L. Glashow, “A Matter - antimatter universe?,” *Astrophys. J.* **495** (1998) 539–549, [arXiv:astro-ph/9707087](#).
  - [2] **Planck** Collaboration, N. Aghanim *et al.*, “Planck 2018 results. I. Overview and the cosmological legacy of Planck,” *Astron. Astrophys.* **641** (2020) A1, [arXiv:1807.06205 \[astro-ph.CO\]](#).
  - [3] B. D. Fields, K. A. Olive, T.-H. Yeh, and C. Young, “Big-Bang Nucleosynthesis after Planck,” *JCAP* **03** (2020) 010, [arXiv:1912.01132 \[astro-ph.CO\]](#). [Erratum: JCAP 11, E02 (2020)].
  - [4] A. D. Sakharov, “Violation of CP Invariance, C asymmetry, and baryon asymmetry of the universe,” *Pisma Zh. Eksp. Teor. Fiz.* **5** (1967) 32–35.
  - [5] G. ’t Hooft, “Symmetry Breaking Through Bell-Jackiw Anomalies,” *Phys. Rev. Lett.* **37** (1976) 8–11.
  - [6] V. A. Rubakov and M. E. Shaposhnikov, “Electroweak baryon number nonconservation in the early universe and in high-energy collisions,” *Usp. Fiz. Nauk* **166** (1996) 493–537, [arXiv:hep-ph/9603208](#).
  - [7] V. A. Kuzmin, V. A. Rubakov, and M. E. Shaposhnikov, “On the Anomalous Electroweak Baryon Number Nonconservation in the Early Universe,” *Phys. Lett. B* **155** (1985) 36.
  - [8] W. Buchmuller and O. Philipsen, “Phase structure and phase transition of the SU(2) Higgs model in three-dimensions,” *Nucl. Phys. B* **443** (1995) 47–69, [arXiv:hep-ph/9411334](#).
  - [9] K. Kajantie, M. Laine, K. Rummukainen, and M. E. Shaposhnikov, “Is there a hot electroweak phase transition at  $m_H \gtrsim m_W$ ?,” *Phys. Rev. Lett.* **77** (1996) 2887–2890, [arXiv:hep-ph/9605288](#).
  - [10] F. Csikor, Z. Fodor, and J. Heitger, “Endpoint of the hot electroweak phase transition,” *Phys. Rev. Lett.* **82** (1999) 21–24, [arXiv:hep-ph/9809291](#).
  - [11] M. Dine and A. Kusenko, “The Origin of the matter - antimatter asymmetry,” *Rev. Mod. Phys.* **76** (2003) 1, [arXiv:hep-ph/0303065](#).
  - [12] D. Bodeker and W. Buchmuller, “Baryogenesis from the weak scale to the grand unification scale,” *Rev. Mod. Phys.* **93** (2021) 035004, [arXiv:2009.07294 \[hep-ph\]](#).
  - [13] D. S. Pereira, J. a. Ferraz, F. S. N. Lobo, and J. P. Mimoso, “Baryogenesis: A Symmetry Breaking in the Primordial Universe Revisited,” *Symmetry* **16** (2024) 13, [arXiv:2312.14080 \[gr-qc\]](#).

- [14] M. Fukugita and T. Yanagida, “Baryogenesis Without Grand Unification,” *Phys. Lett. B* **174** (1986) 45–47.
- [15] M. A. Luty, “Baryogenesis via leptogenesis,” *Phys. Rev. D* **45** (1992) 455–465.
- [16] P. Minkowski, “ $\mu \rightarrow e\gamma$  at a Rate of One Out of  $10^9$  Muon Decays?,” *Phys. Lett. B* **67** (1977) 421–428.
- [17] M. Gell-Mann, P. Ramond, and R. Slansky, “Complex Spinors and Unified Theories,” *Conf. Proc. C* **790927** (1979) 315–321, [arXiv:1306.4669 \[hep-th\]](#).
- [18] T. Yanagida, “Horizontal gauge symmetry and masses of neutrinos,” *Conf. Proc. C* **7902131** (1979) 95–99.
- [19] A. Kusenko, K. Schmitz, and T. T. Yanagida, “Leptogenesis via Axion Oscillations after Inflation,” *Phys. Rev. Lett.* **115** (2015) 011302, [arXiv:1412.2043 \[hep-ph\]](#).
- [20] L. Pearce, L. Yang, A. Kusenko, and M. Peloso, “Leptogenesis via neutrino production during Higgs condensate relaxation,” *Phys. Rev. D* **92** (2015) 023509, [arXiv:1505.02461 \[hep-ph\]](#).
- [21] S. Pascoli, J. Turner, and Y.-L. Zhou, “Baryogenesis via leptonic CP-violating phase transition,” *Phys. Lett. B* **780** (2018) 313–318, [arXiv:1609.07969 \[hep-ph\]](#).
- [22] K. Agashe, P. Du, M. Ekhterachian, C. S. Fong, S. Hong, and L. Vecchi, “Hybrid seesaw leptogenesis and TeV singlets,” *Phys. Lett. B* **785** (2018) 489–497, [arXiv:1804.06847 \[hep-ph\]](#).
- [23] N. D. Barrie, C. Han, and H. Murayama, “Affleck-Dine Leptogenesis from Higgs Inflation,” *Phys. Rev. Lett.* **128** (2022) 141801, [arXiv:2106.03381 \[hep-ph\]](#).
- [24] J. Berman, B. Shuve, and D. Tucker-Smith, “Freeze-in leptogenesis via dark-matter oscillations,” *Phys. Rev. D* **105** (2022) 095027, [arXiv:2201.11502 \[hep-ph\]](#).
- [25] S. Bhattacharya, R. Roshan, A. Sil, and D. Vatsyayan, “Symmetry origin of baryon asymmetry, dark matter, and neutrino mass,” *Phys. Rev. D* **106** (2022) 075005, [arXiv:2105.06189 \[hep-ph\]](#).
- [26] E. Fernández-Martínez, X. Marcano, and D. Naredo-Tuero, “HNL mass degeneracy: implications for low-scale seesaws, LNV at colliders and leptogenesis,” *JHEP* **03** (2023) 057, [arXiv:2209.04461 \[hep-ph\]](#).
- [27] J. Carrasco-Martinez, D. I. Dunsy, L. J. Hall, and K. Harigaya, “Leptogenesis in Parity Solutions to the Strong CP Problem and Standard Model Parameters,” [arXiv:2307.15731 \[hep-ph\]](#).
- [28] A. Datta, R. Roshan, and A. Sil, “Scalar triplet flavor leptogenesis with dark matter,” *Phys. Rev. D* **105** (2022) 095032, [arXiv:2110.03914 \[hep-ph\]](#).
- [29] R. T. Co and K. Harigaya, “Axiogenesis,” *Phys. Rev. Lett.* **124** (2020) 111602, [arXiv:1910.02080 \[hep-ph\]](#).
- [30] Z.-h. Zhao, “Renormalization group evolution induced leptogenesis in the minimal seesaw model with the trimaximal mixing and mu-tau reflection symmetry,” *JHEP* **11** (2021) 170, [arXiv:2003.00654 \[hep-ph\]](#).
- [31] S. Enomoto, C. Cai, Z.-H. Yu, and H.-H. Zhang, “Leptogenesis due to oscillating Higgs field,” *Eur. Phys. J. C* **80** (2020) 1098, [arXiv:2005.08037 \[hep-ph\]](#).
- [32] X.-M. Jiang, Y.-L. Tang, Z.-H. Yu, and H.-H. Zhang, “ $1 \leftrightarrow 2$  processes of a sterile neutrino around the electroweak scale in a thermal plasma,” *Phys. Rev. D* **103** (2021) 095003, [arXiv:2008.00642 \[hep-ph\]](#).
- [33] A. Dutta Banik, R. Roshan, and A. Sil, “Neutrino mass and asymmetric dark matter: study with inert Higgs doublet and high scale validity,” *JCAP* **03** (2021) 037, [arXiv:2011.04371 \[hep-ph\]](#).
- [34] A. Granelli, K. Hamaguchi, N. Nagata, M. E. Ramirez-Quezada, and J. Wada, “Thermal leptogenesis in the minimal gauged  $U(1)_{L_\mu-L_\tau}$  model,” *JHEP* **09** (2023) 079, [arXiv:2305.18100 \[hep-ph\]](#).
- [35] S.-L. Chen, Z. Kang, Z.-K. Liu, and P. Zhang, “Matter Asymmetries in the  $Z_N$  Dark

- matter-companion Models,” [arXiv:2405.05694 \[hep-ph\]](#).
- [36] S. Davidson and A. Ibarra, “A Lower bound on the right-handed neutrino mass from leptogenesis,” *Phys. Lett. B* **535** (2002) 25–32, [arXiv:hep-ph/0202239](#).
- [37] W. Buchmuller, P. Di Bari, and M. Plumacher, “Cosmic microwave background, matter - antimatter asymmetry and neutrino masses,” *Nucl. Phys. B* **643** (2002) 367–390, [arXiv:hep-ph/0205349](#). [Erratum: *Nucl.Phys.B* 793, 362 (2008)].
- [38] W. Buchmuller, P. Di Bari, and M. Plumacher, “A Bound on neutrino masses from baryogenesis,” *Phys. Lett. B* **547** (2002) 128–132, [arXiv:hep-ph/0209301](#).
- [39] W. Buchmuller, P. Di Bari, and M. Plumacher, “The Neutrino mass window for baryogenesis,” *Nucl. Phys. B* **665** (2003) 445–468, [arXiv:hep-ph/0302092](#).
- [40] T. Asaka, K. Hamaguchi, M. Kawasaki, and T. Yanagida, “Leptogenesis in inflaton decay,” *Phys. Lett. B* **464** (1999) 12–18, [arXiv:hep-ph/9906366](#).
- [41] F. Hahn-Woernle and M. Plumacher, “Effects of reheating on leptogenesis,” *Nucl. Phys. B* **806** (2009) 68–83, [arXiv:0801.3972 \[hep-ph\]](#).
- [42] B. Barman, D. Borah, and R. Roshan, “Nonthermal leptogenesis and UV freeze-in of dark matter: Impact of inflationary reheating,” *Phys. Rev. D* **104** (2021) 035022, [arXiv:2103.01675 \[hep-ph\]](#).
- [43] V. Domcke, K. Kamada, K. Mukaida, K. Schmitz, and M. Yamada, “Wash-In Leptogenesis,” *Phys. Rev. Lett.* **126** (2021) 201802, [arXiv:2011.09347 \[hep-ph\]](#).
- [44] V. Domcke, K. Kamada, K. Mukaida, K. Schmitz, and M. Yamada, “Wash-in leptogenesis after axion inflation,” *JHEP* **01** (2023) 053, [arXiv:2210.06412 \[hep-ph\]](#).
- [45] S. Datta, A. Ghosal, and R. Samanta, “Baryogenesis from ultralight primordial black holes and strong gravitational waves from cosmic strings,” *JCAP* **08** (2021) 021, [arXiv:2012.14981 \[hep-ph\]](#).
- [46] B. Barman, D. Borah, S. J. Das, and R. Roshan, “Non-thermal origin of asymmetric dark matter from inflaton and primordial black holes,” *JCAP* **03** (2022) 031, [arXiv:2111.08034 \[hep-ph\]](#).
- [47] R. Calabrese, M. Chianese, J. Gunn, G. Miele, S. Morisi, and N. Saviano, “Limits on light primordial black holes from high-scale leptogenesis,” *Phys. Rev. D* **107** (2023) 123537, [arXiv:2305.13369 \[hep-ph\]](#).
- [48] K. Schmitz and X.-J. Xu, “Wash-in leptogenesis after the evaporation of primordial black holes,” [arXiv:2311.01089 \[hep-ph\]](#).
- [49] A. Ghoshal, Y. F. Perez-Gonzalez, and J. Turner, “Superradiant Leptogenesis,” [arXiv:2312.06768 \[hep-ph\]](#).
- [50] D. Suematsu, “Low scale leptogenesis in a hybrid model of the scotogenic type I and III seesaw models,” *Phys. Rev. D* **100** (2019) 055008, [arXiv:1906.12008 \[hep-ph\]](#).
- [51] P. Huang and T. Xu, “Leptogenesis with a Coupling Knob,” [arXiv:2312.06380 \[hep-ph\]](#).
- [52] E. J. Chun, T. P. Dutka, T. H. Jung, X. Nagels, and M. Vanvlasselaer, “Bubble-assisted leptogenesis,” *JHEP* **09** (2023) 164, [arXiv:2305.10759 \[hep-ph\]](#).
- [53] M. Dehpour, “Thermal leptogenesis in nonextensive cosmology,” *Eur. Phys. J. C* **84** (2024) 340, [arXiv:2401.00229 \[hep-ph\]](#).
- [54] M. Dehpour, “Thermal leptogenesis in anisotropic cosmology,” *Int. J. Mod. Phys. A* **38** (2023) 2350181, [arXiv:2312.10677 \[hep-ph\]](#).
- [55] A. Pilaftsis and T. E. J. Underwood, “Resonant leptogenesis,” *Nucl. Phys. B* **692** (2004) 303–345, [arXiv:hep-ph/0309342](#).
- [56] A. Pilaftsis, “Resonant tau-leptogenesis with observable lepton number violation,” *Phys. Rev. Lett.* **95** (2005) 081602, [arXiv:hep-ph/0408103](#).
- [57] B. Dev, M. Garny, J. Klaric, P. Millington, and D. Teresi, “Resonant enhancement in

- leptogenesis,” *Int. J. Mod. Phys. A* **33** (2018) 1842003, [arXiv:1711.02863 \[hep-ph\]](#).
- [58] P. C. da Silva, D. Karamitros, T. McKelvey, and A. Pilaftsis, “Tri-resonant leptogenesis in a seesaw extension of the Standard Model,” *JHEP* **11** (2022) 065, [arXiv:2206.08352 \[hep-ph\]](#).
- [59] D. Karamitros, T. McKelvey, and A. Pilaftsis, “Varying entropy degrees of freedom effects in low-scale leptogenesis,” *Phys. Rev. D* **109** (2024) 055007, [arXiv:2310.03703 \[hep-ph\]](#).
- [60] Z.-h. Zhao, J. Zhang, and X.-Y. Wu, “Flavored leptogenesis from a sudden mass gain of right-handed neutrinos,” [arXiv:2403.18630 \[hep-ph\]](#).
- [61] R. Barbieri, P. Creminelli, A. Strumia, and N. Tetradis, “Baryogenesis through leptogenesis,” *Nucl. Phys. B* **575** (2000) 61–77, [arXiv:hep-ph/9911315](#).
- [62] A. Abada, S. Davidson, A. Ibarra, F. X. Josse-Michaux, M. Losada, and A. Riotto, “Flavour Matters in Leptogenesis,” *JHEP* **09** (2006) 010, [arXiv:hep-ph/0605281](#).
- [63] K. Moffat, S. Pascoli, S. T. Petcov, H. Schulz, and J. Turner, “Three-flavored nonresonant leptogenesis at intermediate scales,” *Phys. Rev. D* **98** (2018) 015036, [arXiv:1804.05066 \[hep-ph\]](#).
- [64] T. Alanne, T. Hugle, M. Platscher, and K. Schmitz, “Low-scale leptogenesis assisted by a real scalar singlet,” *JCAP* **03** (2019) 037, [arXiv:1812.04421 \[hep-ph\]](#).
- [65] P. S. B. Dev, R. N. Mohapatra, and Y. Zhang, “Leptogenesis constraints on  $B - L$  breaking Higgs boson in TeV scale seesaw models,” *JHEP* **03** (2018) 122, [arXiv:1711.07634 \[hep-ph\]](#).
- [66] D. M. Barreiros, H. B. Câmara, R. G. Felipe, and F. R. Joaquim, “Scalar-singlet assisted leptogenesis with CP violation from the vacuum,” *JHEP* **01** (2023) 010, [arXiv:2211.00042 \[hep-ph\]](#).
- [67] J. A. Casas and A. Ibarra, “Oscillating neutrinos and  $\mu \rightarrow e, \gamma$ ,” *Nucl. Phys. B* **618** (2001) 171–204, [arXiv:hep-ph/0103065](#).
- [68] B. Pontecorvo, “Inverse beta processes and nonconservation of lepton charge,” *Zh. Eksp. Teor. Fiz.* **34** (1957) 247.
- [69] Z. Maki, M. Nakagawa, and S. Sakata, “Remarks on the unified model of elementary particles,” *Prog. Theor. Phys.* **28** (1962) 870–880.
- [70] **Particle Data Group** Collaboration, R. L. Workman and Others, “Review of Particle Physics,” *PTEP* **2022** (2022) 083C01.
- [71] M. C. Gonzalez-Garcia, M. Maltoni, and T. Schwetz, “NuFIT: Three-Flavour Global Analyses of Neutrino Oscillation Experiments,” *Universe* **7** (2021) 459, [arXiv:2111.03086 \[hep-ph\]](#).
- [72] S. Antusch, P. Di Bari, D. A. Jones, and S. F. King, “Leptogenesis in the Two Right-Handed Neutrino Model Revisited,” *Phys. Rev. D* **86** (2012) 023516, [arXiv:1107.6002 \[hep-ph\]](#).
- [73] L. Covi, E. Roulet, and F. Vissani, “CP violating decays in leptogenesis scenarios,” *Phys. Lett. B* **384** (1996) 169–174, [arXiv:hep-ph/9605319](#).
- [74] S. Y. Khlebnikov and M. E. Shaposhnikov, “The Statistical Theory of Anomalous Fermion Number Nonconservation,” *Nucl. Phys. B* **308** (1988) 885–912.
- [75] E. W. Kolb and M. S. Turner, *The Early Universe*, vol. 69. 1990.
- [76] Z.-Z. Xing and S. Zhou, *Neutrinos in particle physics, astronomy and cosmology*. Springer, 2011.
- [77] E. W. Kolb and S. Wolfram, “Baryon Number Generation in the Early Universe,” *Nucl. Phys. B* **172** (1980) 224. [Erratum: *Nucl.Phys.B* 195, 542 (1982)].
- [78] W. Buchmüller, P. Di Bari, and M. Plumacher, “Leptogenesis for pedestrians,” *Annals Phys.* **315** (2005) 305–351, [arXiv:hep-ph/0401240](#).
- [79] P. Gondolo and G. Gelmini, “Cosmic abundances of stable particles: Improved analysis,” *Nucl. Phys. B* **360** (1991) 145–179.
- [80] M. Plumacher, “Baryon asymmetry, neutrino mixing and supersymmetric SO(10) unification,”

*Nucl. Phys. B* **530** (1998) 207–246, [arXiv:hep-ph/9704231](https://arxiv.org/abs/hep-ph/9704231).